2

Fundamentals of Clays

Surface and Colloid Science, and Rheology

Elizaveta Forbes and Andrew Chryss

2.1 Introduction

Relating bulk properties of clays and clay suspensions to their particle morphology or surface chemistry is a complex process due to the multiple possible types of interaction and the large number of bodies over which these forces act. The work that has been done on simple, idealized suspensions can be extended to complex multi-component suspensions, such as clay in water, with caution. This allows the observation of trends in behaviour to be given some meaning and predictions to be made. This chapter combines the surface and colloid science with macroscopic rheological behaviour due to the strong causal relationships involved. For example, what affects clay swelling behaviour also affects the rheology, and the swelling itself leads to complex rheological behaviour.

2.2 Mineral Structure

2.2.1 Silicate Minerals

Silicate minerals are by far the most commonly occurring minerals in the world. All silicate minerals are based on tetrahedral building blocks. These tetrahedral units are composed of a central Si^{4+} atom bonded to four surrounding O^{2-} atoms, more commonly known as the silica tetrahedron.

Different families of silicate minerals are based upon the numerous ways in which these tetrahedra may be combined (Klein and Hurlbut, 1993), either as isolated tetrahedra (e.g. olivine), single or double chains of tetrahedra (e.g. orthopyroxene, hornblende), as an interlocking tetrahedral framework (e.g. feldspar, quartz), or as tetrahedral sheets (e.g. talc, kaolinite). The different combinations of tetrahedral blocks are illustrated in Fig. 2.1. This review focuses on the phyllosilicate mineral family, as all clay minerals fall within this family (Deer *et al.*, 1992).

2.2.2 Phyllosilicate Minerals

Phyllosilicate minerals are so named because the sheets of silica tetrahedral tend to give the minerals a platy/leafy habit, as illustrated in an SEM image in Fig. 2.2.

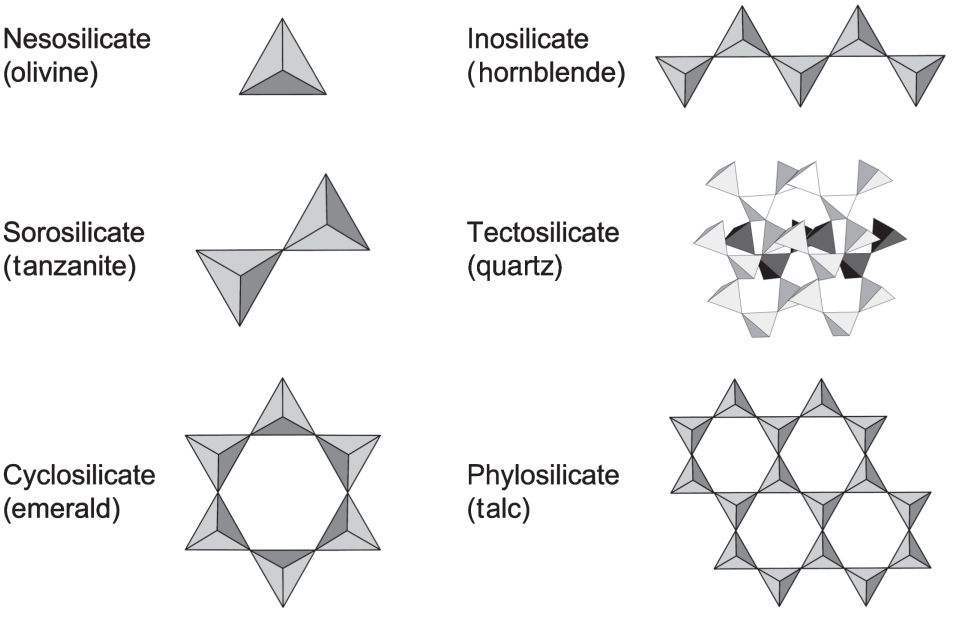

Figure 2.1. Types of silicates (Deer *et al.*, 1992).

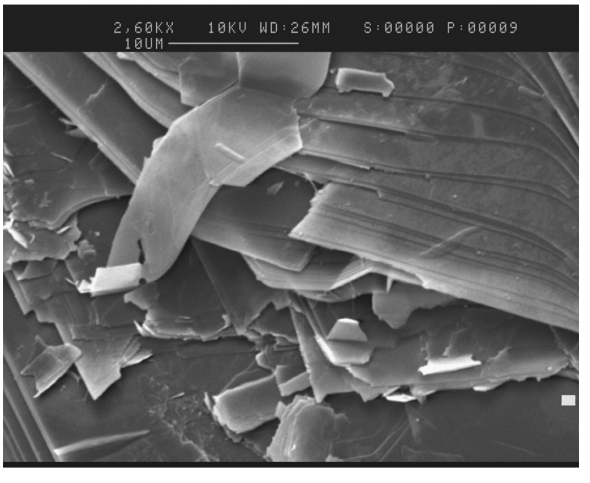

Figure 2.2. Plate-like smectite particles. Image courtesy of Angus McFarlane.

There are a large number of different types of phyllosilicates in existence with a variety of different properties. The detailed structure of phyllosilicates is composed of a combination of tetrahedral and octahedral sheets. Individual octahedra are made up of two layers of four oxygen/hydroxyl atoms, with embedded magnesium or aluminium atoms arranged in an octahedral coordination, as illustrated in Fig. 1.4 and already discussed in Chapter 1.

The variation of the stacking of the tetrahedral (T) and octahedral (O) sheets makes up the different types of phyllosilicate minerals. The way in which these minerals are subclassified is not uniform across the literature. For the purposes of this review the taxonomic approach taken is that as outlined in Table 1.1, i.e. (1) type, (2) group, (3) subgroup and (4) species. While in practical consideration of the mineral processing value chain (MPVC) most of the review concentrates on the kaolinite and smectite groups as illustrative 1:1 and 2:1 clays, it would be erroneous to assume that the deleterious effects often seen in industrial practice are limited to the minerals within these two groups. In fact, minerals such as talc and serpentine often get clustered together with kaolinite (and other swelling and non-swelling clays), and are generically referred to as 'clay minerals'. The disparity in the terminology used to describe deleterious minerals often leads to confusion with regards to what constitutes a 'clay mineral' or a 'clay'.

It would be more correct to say that the common use of the term 'clay minerals' refers to phyllosilicates in general. Within the phyllosilicates, different groups contain minerals that have different degrees to which they affect the behaviour of ore slurries, ranging from mild to extreme. The clay mineral that arguably exhibits the most extreme behaviour of all (chrysotile) belongs to the serpentine group, not the 'clay' group as normally perceived.

2.2.2.1 Talc and Chlorite Groups

Talc and chlorite are largely similar in structure, both consisting of a three-layered T–O–T structure. In the case of talc, the sheets are held together by weak van der Waals forces and easily come apart when ground. The resulting particles tend to be smooth platelets, commonly used in paints, coatings and cosmetics. In the case of chlorite, the T–O–T sheets are similar to that of talc, but separated by an extra octahedral brucite layer (Deer *et al.*, 1992).

Talc and chlorite minerals occur as gangue components of many base metal sulphide ore deposits around the world (Schouwstra *et al.*, 2000). These ores are generally beneficiated by means of the flotation process. Due to natural floatability, talc and chlorite readily enter the flotation concentrates, reducing their grade.

2.2.2.2 Mica Group

The continuous stacking of consecutive T–O–T units results in the thin, platy morphology of minerals such as muscovite. The space between the T–O–T layers is occupied by interlayer cations. The two most prevalent mica types, biotite and muscovite, are characterized by K^+ ions in their interlayers (Deer *et al.*, 1992). In this, micas are more similar to swelling clays than to talc. In fact, micas serve as precursors to swelling clays such as vermiculites and smectites. The transformation of micas to swelling clays is well documented (Bracke *et al.*, 1995; Churchman, 1980) and occurs as a result of the replacement of the

non-exchangeable interlayer cations by exchangeable hydrated cations. This exchange of cations occurs as a result of weathering within the mineral deposits.

2.2.2.3 Kaolinite and Smectite Groups

This group is the more commonly perceived 'clays'; kaolinite in particular is commonly known as 'pottery clay'. These minerals are commonly used in ceramics, as well as paints and coatings applications.

Minerals in this group can be further classified into the swelling (smectite) and non-swelling (kaolinite) varieties. The capacity to swell originates from the interlayer cations found between the T–O–T sheets of these minerals. The interlayer cations are typically strongly hydrated ions (Mg^{2+}, Ca^{2+}). These ions attract water molecules that accumulate between the sheet layers of minerals such as montmorillonite or smectite, forcing the adjoining sheets apart and causing the mineral to swell. The degree of swelling is determined by the hydration capacity of the interlayer cations (Klein and Hurlbut, 1993; Luckham and Rossi, 1999). The swelling leads to an effective increase in the volumetric solids fraction of the suspensions, which in turn leads to an increase in particle–particle interactions and complex rheological behaviour.

Suspensions containing swelling clay minerals such as montmorillonite present substantial dewatering and impoundment challenges in tailings treatment due to their low settling and poor compaction rates (McFarlane *et al.*, 2005). Problems associated with swelling clays are commonly encountered in the processing of coal, phosphate and bauxite industries (de Kretser *et al.*, 1997; Power *et al.*, 2011; Sofrá and Boger, 2002).

2.2.2.4 Serpentine Group

The serpentine group requires a closer inspection, as the minerals within it can deviate from the more common platy habit and form fibrous or corrugated structures. This deviation is caused by the mismatch of bond lengths between the octahedral and tetrahedral units. The T–O structure of serpentine minerals is very similar to that of kaolinite (see Fig. 1.4). In the case of kaolinite, the octahedral unit contains aluminium atoms, and the bond length between the octahedral and tetrahedral sheets is well matched. For this reason, kaolinite particles form distinct platelets. However, when the octahedral unit contains magnesium ions, the bond length in the octahedral unit is slightly shorter than that of the tetrahedral unit. This is the case with minerals such as antigorite and chrysotile. In order to compensate for the bond length mismatch, the entire structure begins to curve (Mellini and Zanazzi, 1987; Yada, 1971).

In the case of antigorite, this results in a corrugated configuration. In the case of chrysotile (often termed 'asbestos'), the plates roll up into tight tubes. These tubes then take the form of long, thin fibres, which result in extremely problematic behaviour when present in mineral processing streams (Burdukova *et al.*, 2008; Ndlovu *et al.*, 2011; Ralston and Fornaserio, 2006; Senior and Thomas, 2005). The morphology of chrysotile is illustrated in Fig. 2.3. This bond length mismatch does not cause similar curving behaviour in other magnesium-based phyllosilicates, as the presence of the second tetrahedral layer (T–O–T configuration) tends to balance out the structure.

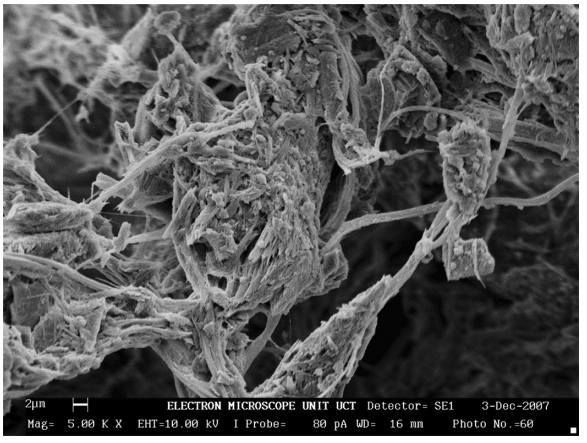

Figure 2.3. SEM of chrysotile fibres.

2.3 The Electrical Double Layer and Inter-Particle Forces

When discussing the impact of clay minerals on mineral processing operations, one generally refers to their behaviour in aqueous suspension, i.e. as a mineral slurry. When minerals are present in an aqueous environment, they become subject to different inter-particle forces, which then have a strong impact on the macroscopic flow properties of these same suspensions. The types of forces acting between mineral particles and the impact this has on particle–particle interactions are summarized below.

2.3.1 DLVO Theory

DLVO theory was independently developed by Derjaguin and Landau (1941) and Verwey and Overbeek (1948). Although Derjaguin's paper was published first, both sets of authors are given equal credit for the theory, as the intervening years cover the duration of the Second World War.

The theory states that the overall total force between two particles in aqueous suspension is determined by the balance of attractive and repulsive forces, as outlined in Eq. (2.1).

$$F_{Tot} = F_{attractive} - F_{repulsive} \tag{2.1}$$

In the classic DLVO theory, the forces responsible for the attraction are the attractive van der Waals force and heterocoagulation, while the repulsive force is attributed to double-layer repulsion (Hogg *et al.*, 1966). However, the theory was later revised to include the attractive hydrophobic force and the repulsive steric force. The nature of these surface forces has been described in great detail by a number of authors (Adamson, 1985; Dukhin and Derjaguin, 1976; Gregory, 2006; Hiemenz and Rajagopolan, 1997; Hunter, 1988; Israelachvili, 1985), and only a brief overview will be presented here.

2.3.1.1 Van der Waals Force

The van der Waals force arises due to the interaction between polarizable molecules or molecules and a surface. For two spherical particles, the force can be expressed in terms of Eq. (2.2), where a is the particle radius, H is the distance between particles, and A_H is the Hamaker constant. The van der Waals attraction has a short range and comes into play if the distance H is significantly smaller than the particle radius (typically 1–10 nm) (Israelachvili and Pashley, 1983).

$$F_{VDW} = -\frac{aA_H}{12H^{12}} \tag{2.2}$$

2.3.1.2 Double-Layer Repulsion

When mineral particles are placed in aqueous solution, they typically acquire a strong electrical charge. The presence of the surface charge causes the ions in solution to become re-distributed around the mineral particle. The oppositely charged counter-ions form an inner layer close to the particle surface, called the adsorbed layer. Another, less concentrated layer of co- and counter-ions forms the outer shell, known as the diffuse layer. The concentration of counter-ions decreases with an increasing distance away from the particle surface, until it reaches that of the bulk solution. This double-layer model is illustrated in Fig. 2.4 (Dukhin and Derjaguin, 1976).

The charge potential of the particle surface is commonly approximated by the zeta potential (ζ), which is the charge potential on the outer plane of the adsorbed layer, also known as the Stern plane. The thickness of the double layer is termed the Debye length (κ^{-1}) and is a strong function of the ionic strength of the aqueous medium (I), as shown in Eq. (2.3). Hence the range of the repulsion can vary significantly depending on the electrolyte concentration in the bulk solution.

When two similarly charged particles are brought together, the double layers around the particles begin to overlap, causing the concentration of ions between the two surfaces to be greater than of the bulk aqueous medium. The decrease in the entropy and the increase in the osmotic pressure result in the formation of a repulsive force between the two particles, as described by Eq. (2.4), where H is the distance from the surface, ζ is the zeta potential, ε is the dielectric constant of the bulk solution and ε_0 is the permittivity of free space.

$$\kappa^{-1} \propto \frac{1}{\sqrt{I}} \tag{2.3}$$

$$F_{ELD} = \frac{2\pi a\varepsilon_0\varepsilon\kappa\zeta^2 e^{-\kappa H}}{1+e^{-\kappa H}} \tag{2.4}$$

The zeta potential of the particles can be altered by the varying concentrations of potential determining ions in the bulk solution. For oxide minerals, potential is determined by H^+ and OH^- ions, i.e. the solution pH.

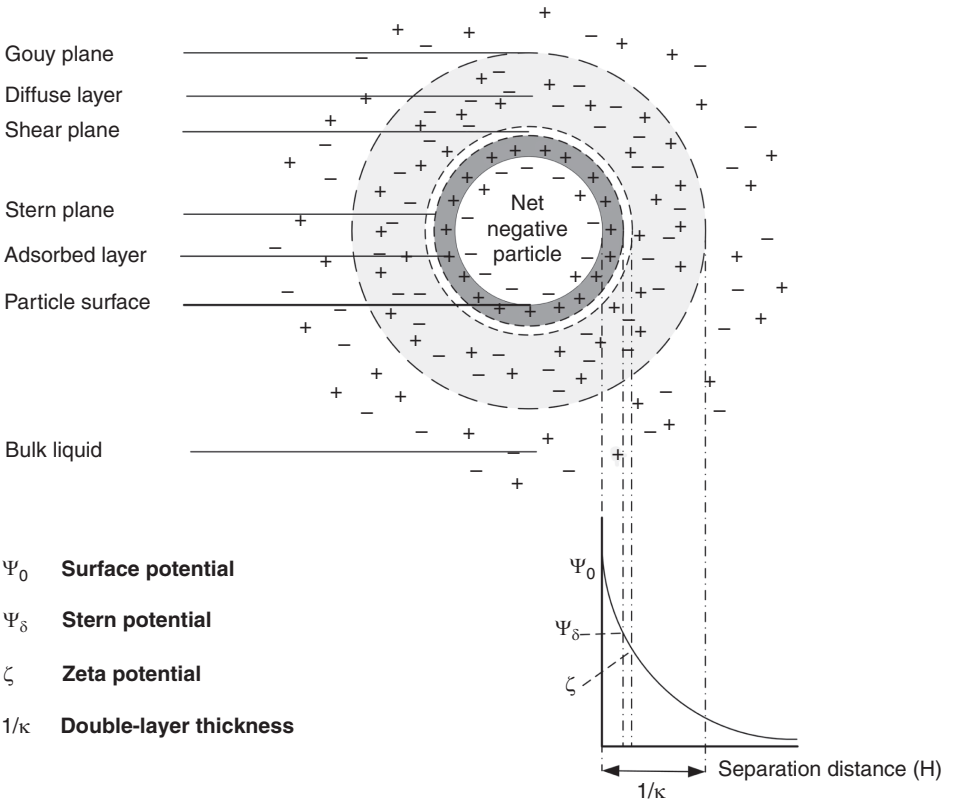

Figure 2.4. Theoretical structure of the electrical double layer.

2.3.1.3 Hydrophobic Attraction

The nature and the existence of the hydrophobic force are still debated. The concept of hydrophobic attraction gained prominence when it was discovered that in the case of non-polar solids, the magnitude of the long-range attractive force could not be explained by means of classic DLVO theory. The early work of Israelachvili and Pashley (1983) showed that when two such surfaces are in close proximity in water, there is a strong attraction between them. This and other early work mainly found it to be a short-range attraction, similar to that of the van der Waals force (in the order of 1–10 nm) (Israelachvili and Pashley, 1983; Meagher and Craig, 1994; Pashley *et al.*, 1985). Later investigations found the attraction had a significantly longer range, with estimates varying from 20 to 300 nm (Craig *et al.*, 1998, 1999; Ishida *et al.*, 2000a; Kurihara *et al.*, 1990; Mantel *et al.*, 1995; Rabinovich and Derjaguin, 1988).

Many researchers now believe that the long-range component of hydrophobic attraction is mainly due to nano-bubbles present on the hydrophobic surfaces (Ishida *et al.*, 2000b), which can bridge a gap of a few hundred nanometres between the surfaces and create

capillary adhesion (Ishida *et al.*, 2000a; Meyer *et al.*, 2006). Nano-bubbles would only be expected when there is a 'supply' of air to the surface, such as when the surface is inserted into the liquid from air or when solvent conditions are changed so that bubbles nucleate on the surface (Zhang *et al.*, 2008). The current estimate of the range of the 'true' hydrophobic attraction is between 1 and 10 nm, and the exact nature of this attraction is still not fully understood (Meyer *et al.*, 2006).

2.3.1.4 Steric Repulsion

In mineral processing operations, steric repulsion occurs as a result of the presence of molecular species on the mineral surfaces. These molecules are typically water-soluble polymers of a short to medium chain length. While longer chain polymers (such as typical flocculants) cause particles to aggregate through bridging, shorter chain polymers can instead cause the suspension to become dispersed.

This dispersion can take place through two mechanisms. When two polymer-coated surfaces are brought together, the overall polymer concentration between the two surfaces increases, creating an increase in the osmotic pressure existing between the two surfaces. In addition, the compression of the extended polymer molecules results in an elastic force, creating additional resistance to contact (Laskowski and Pugh, 1992). In the case where the polymers themselves carry an electrical charge, an additional component of the repulsive force can be present due to the enhancement of double-layer repulsion with the additional polymer charge (Marra and Hair, 1988).

2.4 Clay Particles in Aqueous Suspension

2.4.1 Anisotropic Nature of Phyllosilicate Particles

Because of the platy habits of phyllosilicate minerals, phyllosilicate particles possess distinct basal faces and edges. The different particle planes have different surface charge characteristics, causing the particles to become charge anisotropic. As a result, these particles display distinctly different behaviour from the more uniformly charged isotropic minerals (such as quartz or galena), and have complex modes of particle–particle association, which change depending on the surface charge distribution of the different particle facets, which in turn is dependent upon solution pH. The exact nature of these modes of association is still debated in the literature, with no uniform consensus. The edge versus basal interaction is critically important in the coagulation and flocculation behaviour of clays, and this is addressed in detail in Chapter 8.

Early research into clay minerals proposed that the tetrahedral basal planes of phyllosilicates carry a permanent negative charge due to the isomorphous substitutions of Si^{4+} ions in the tetrahedral layer with metal ions (such as Al^{3+} and Ti^{3+}). The presence of lower valence metal ions causes a charge imbalance in the tetrahedral plane, leaving the faces with a permanent negative charge (Schofield and Samson, 1954; Swartzen-Allen and Matijevic, 1974; van Olphen, 1951).

On the other hand, other researchers argue that the magnitude of ion substitution was insufficient to cause the negative charge behaviour of tetrahedral basal plane surfaces (Nishimura *et al.*, 1995; Scales *et al.*, 1990). They propose that basal plane (face) charge is not constantly negative, but is instead strongly pH dependent, with an isoelectric point at pH 2. These assertions are made based on the use of zeta potential and streaming potential techniques. The authors used their findings to conclude that the pH-dependant nature of the basal plane surfaces was a result of the hydrolysis of the Si–O–Si sites, making the surface charge of tetrahedral planes similar to that of quartz. The simplest way to view the basal faces are as areas dominated by silanol groups with a negative charge over most of the pH range.

The edge faces of phyllosilicates are more complex because of the role of aluminol as well as silanol groups, and are thought to carry a charge that changes from positive (low pH) to negative (high pH) as a function of pH. This charge arises from the presence of amphoteric hydroxyl sites on the edge surface: SiO sites in the tetrahedral portion and the AlO/MgO sites in the octahedral portion of the particle edge (Johnson *et al.*, 1998; Tombácz and Szekeres, 2006; Williams and Williams, 1977).

These surface sites are amenable to protonation/deprotonation by H^+ and OH^- ions in a manner illustrated in Eq. (2.5). For this reason H^+ and OH^- ions are often referred to as 'potential determining ions' and this mechanism is responsible for the alteration of mineral surface charge with pH (see also Fig. 8.5).

$$H_2O + MO^- \underset{OH^-}{\overset{H^+}{\rightleftharpoons}} MOH \underset{OH^-}{\overset{H^+}{\rightleftharpoons}} MOH_2^+ \tag{2.5}$$

2.4.2 Charge Measurement for Anisotropic Particles

The exact measurement of the surface charge characteristics of both the basal faces and edge faces of clay particles is exceedingly difficult. Before surface (force) specific microscopy techniques (such as atomic force microscopy (AFM)) became available, attempts to quantify the surface charge of anisotropic minerals relied on bulk (or average) measurements. Such techniques cannot measure the charge on isolated surface planes and therefore require extensive interpretation, which can often lead to misleading results.

2.4.2.1 Zeta Potential

One of the more controversial techniques for charge magnitude estimation is the use of zeta potential measurements. Zeta potential is commonly calculated by means of measuring the mobility of a particle in suspension within an electric field (electrophoretic mobility). The resultant zeta potential estimate is then treated as a close approximation of surface potential.

The use of zeta potential measurements with regards to clay minerals can be problematic. Since the minerals are anisotropic, the mobility of the particles in the aqueous medium represents an 'apparent' value that is (at best) an average zeta potential of all the particle planes. Furthermore, the value of zeta potential measurements is strongly dependent on the

thickness of the electrical double layer, which in turn is dependent on the concentration of electrolyte in solution. Some researchers feel that this added complexity further invalidates zeta potential as an accurate proxy for surface potential (Hou *et al.*, 2009).

Several authors have attempted to 'deconstruct' the average zeta value using an estimate of the particle aspect ratio, i.e. the relative surface areas of differently charged planes (Johnson *et al.*, 1998; Williams and Williams, 1977). These studies indicate that the overall zeta potential of clay minerals strongly resembled that of quartz, which was used to conclude that the negatively charged tetrahedral (basal) faces dominate the overall charge of the particle surfaces. This approach relies heavily on the assumption that clay particles occur as perfect crystalline units, which has since been shown to be incorrect (Du *et al.*, 2010; Żbik *et al.*, 2008).

Conversely, a number of studies have looked at the surface potential of talc, with an incorrect underlying assumption that that talc basal planes are perfectly charge compensated and therefore neutral. The zeta potential measurements were then assumed to represent the surface potential of talc edges (Bremmell and Addai-Mensah, 2005; Fuerstenau and Huang, 2003; Fuerstenau *et al.*, 1988; Steenberg and Harris, 1984).

These instances highlight the fact that the use of zeta potential measurements to estimate the surface charge distribution of anisotropic minerals can be highly misleading and certain researchers advise to avoid it altogether when working with anisotropic clay minerals (Burdukova *et al.*, 2007; Hou *et al.*, 2009; Missana and Adell, 2000). Nonetheless, there are ways in which zeta potential measurements can be used to estimate the way in which clay minerals can interact with other minerals on the basis of charge. This is specifically pertinent in determining whether clay minerals are likely to cause 'slime coatings' in flotation applications (Arnold and Aplan, 1986; Attia and Deason, 1989; Fuerstenau *et al.*, 1958; Iwasaki *et al.*, 1962).

One such method makes use of the distribution of zeta potential measurements in a binary mineral system (Liu *et al.*, 2002; Xu *et al.*, 2003). The measurement involves obtaining the zeta distribution of each individual mineral and then compares it to the zeta distribution of a binary mineral mixture. This technique can give an indication of whether or not one of the minerals had been effectively coated with another (a single distribution peak vs a bimodal distribution). This method does not estimate the exact nature of the clay surface charge, but it does provide a measure that can predict the behaviour of that mineral in an industrial setting.

2.4.2.2 Streaming Potential

A method similar to zeta potential measurements, though more restricted, is that of streaming potential. In this technique, a particle is not freely suspended in the aqueous medium, but rather a single mineral plate is exposed to the surrounding liquid (Nalaskowski *et al.*, 2007; Scales *et al.*, 1990). This approach typically requires a relatively large, isolated basal plane surface, which is very difficult to obtain in practice. Of all the phyllosilicate minerals, the only one that is amenable to obtaining perfectly cleaved flakes large enough to perform such measurements is mica. Surface streaming potential studies are thus confined

to studying mica surfaces and not those of other minerals. Furthermore, streaming potential measurements are subject to the same scepticism as zeta potential measurements when it comes to using them as adequate proxies for surface potential measurements, and has been strongly questioned (Hou *et al.*, 2009; Missana and Adell, 2000).

2.4.2.3 Potentiometric Titrations

The use of titrations to study the surface charge distribution is one of the more widely accepted and implemented methodologies (Burdukova *et al.*, 2007; Duc *et al.*, 2005a, 2005b; Tombácz and Szekeres, 2004, 2006; Zhao *et al.*, 2008). The technique involves estimating the net surface charge density of minerals through the exchange between potential determining ions (H^+ and OH^-) and ions of an indifferent electrolyte (e.g. NaCl) on the mineral surface (Laskowski and Sobieraj, 1969; Mular and Roberts, 1966). The magnitude of the surface charge density can be calculated using Eq. (2.6), where σ_0 is the net surface charge density, F is the Faraday constant and γ_i is the adsorption density of potential determining ions (Hunter, 1988).

$$\sigma_0 = \mathrm{F} \cdot \left(\gamma_{H^+} - \gamma_{OH^-} \right) \tag{2.6}$$

When indifferent electrolyte is present in solution, the overall ionic strength of that solution increases. This causes the electrical double layer to become compressed, resulting in a shorter Debye length (see Eq. (2.3)). As a result, the value of the Stern Potential (Ψ_S) decreases (see Fig. 2.4). This in turn causes potential determining ions to be adsorbed onto the surface in order to compensate for the change. The adsorption of these ions from solution is then reflected in the overall solution pH. Therefore, the net surface potential can be measured by measuring the change in solution pH as a function of an increase in the concentration of background electrolyte, as illustrated in Fig. 2.5. Unlike zeta potential and streaming potential measurements, this technique gives a direct estimate of surface charge that is not dependent on the thickness of the electrical double layer.

The obtained point of zero charge (pzc) is thought to represent the net point of zero charge (NPZC) of all the pH dependent mineral facets (i.e. broken ion sites subject to adsorption and desorption of H^+ and OH^- ions). Several researchers believe that this NPZC represents the NPZC of the edge surfaces only (Janek and Lagaly, 2001; Penner and Lagaly, 2001; Tombácz and Szekeres, 2004, 2006). This stance rests on the assumption that the tetrahedral basal planes of clay minerals carry a permanent/constant negative charge that is present entirely due to the isomorphic ion substitution into the tetrahedra and is therefore pH independent (van Olphen, 1951). This means that the potentiometric titration results can be used to estimate the surface charge density of clay particle edges as a function of pH.

However, as was mentioned in the previous sections, not all researchers believe that the surface charge of the tetrahedral basal planes is pH independent (Nishimura *et al.*, 1995; Scales *et al.*, 1990). If this is the case, then potentiometric titration measurements are subject to the same uncertainty as zeta potential measurements, where only an average or 'apparent' charge distribution can be obtained using the technique. On the other hand, the very

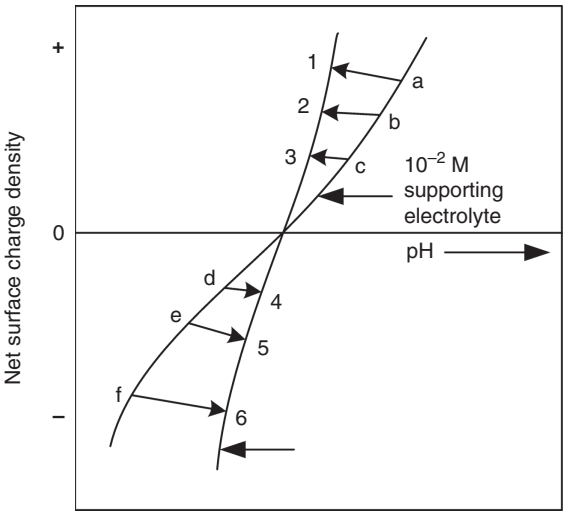

Figure 2.5. Schematic representation of a potentiometric titration (Mular and Roberts, 1966).

assertion that the basal plane surfaces are pH dependant is based on zeta potential measurements, which many researchers believe are inappropriate. This means that many of the arguments with regards to the validity of various techniques can rapidly become circular.

2.4.2.4 Microscopic Methods

Recent advances in the field of AFM technology have enabled researchers to look directly at the specific particle planes and directly measure the surface charge distribution (Nalaskowski *et al.*, 2007; Zhao *et al.*, 2008). The results of the studies have largely confirmed the existing notions of the surface charge distributions – that the basal planes are not pH dependent and the edge charges agreed with estimates generated by titration measurements. The difference is dramatically illustrated in Fig. 2.6.

Exact magnitudes of the basal face and edge face charges are still difficult to measure, in part as it is exceedingly difficult to obtain a sufficiently smooth surface on which to perform the measurements. However, in more recent years improved estimates of surface-specific surface potentials have begun to emerge (Yan *et al.*, 2011; Yin *et al.*, 2012). These measurements once more confirm the presence of the consistently negative charge of the basal plane surfaces, which corroborates the hypothesis of the isomorphous substitution as the source of the negative charge.

2.5 Models of Particle Interactions

The charge disparity between particle basal and edge faces means that the simple model of an electrical double layer that holds for a largely symmetric, uniformly charged mineral particle cannot be applied to an anisotropic particle. In the case of simple isotropic

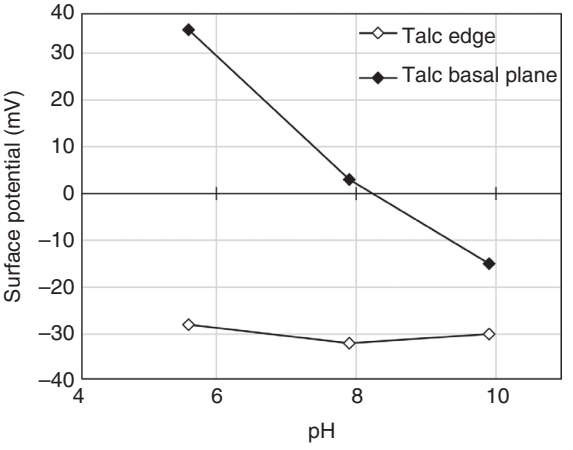

Figure 2.6. Surface potentials of basal planes and edges of talc (from reported data in Yin *et al.*, 2012)

particles, the double-layer forces are always repulsive, since the particles are similarly charged. The net inter-particle forces usually become attractive at a point where the overall surface charge of the particle is zero, and the attractive van der Waals forces become dominant.

This simple model does not hold for anisotropic particles, where different particle faces carry a different electrical charge. These differently charged faces will interact via electrical double-layer forces in such a way that the oppositely charged surfaces result in an attractive force (Hogg *et al.*, 1966). As a result, interactions between particles of the same clay mineral are often described in the form of complex particle–particle coordinations. Van Olphen (1951) first proposed that there are three main types of particle–particle interactions between anisotropic clay particles: face–face (FF), face–edge (EF) and edge–edge (EE), as illustrated in Fig. 2.7. These interactions are thought to arise from the differences in the electrical charge of the basal plane and edge surfaces at a given pH.

Van Olphen (1951) postulated that at a pH when both the basal planes and edges of particles carry a negative charge, the overall inter-particle forces would be repulsive, resulting in a randomly dispersed particle orientation (Fig. 2.7a). This would typically take place at high pH values. However, as pH decreases, the charge on the particle edges would begin to decrease, approaching a point of zero charge. At this point the dominant force between particle edges would be the attractive van der Waals force, while the force between negatively charged particle planes would remain a strongly repulsive double-layer force. This would cause the particles to coagulate in the EE configuration (Fig. 2.7d).

As the pH decreases further, and the charge on the particle edge faces becomes positive, an attractive force develops between negatively charged basal planes and positively charged edges, engendering a ‘house of cards’ type particle interaction (Fig. 2.7c).

Face–face coagulation is slightly more complex, as it could take place in two ways depending on the structure of the mineral. The T–O–T structured minerals (e.g. montmorillonite)

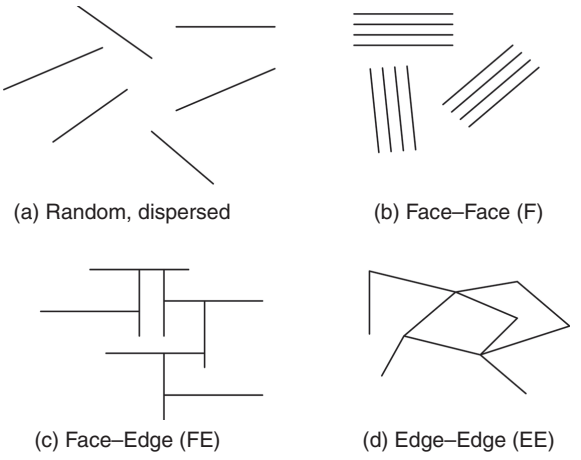

Figure 2.7. Possible orientation of clay particles (van Olphen, 1951).

have two identical basal planes. This means that in order for FF coagulation to take place, the negative charge on the basal planes needs to approach zero, in order for attractive van der Waals forces to become dominant. On the other hand, minerals like kaolinite, which have a T–O structure, have two types of basal plane surface. One is a permanently negative tetrahedral face, while the other is an octahedral face with a surface charge that alters as a function of pH. The coagulation between these surfaces can therefore occur as a result of an attractive force between two oppositely charged basal plane surfaces.

Although a large number of authors adhere to van Olphen's original propositions (Du *et al.*, 2010; Kitchener, 1969; Rand and Melton, 1975; Schofield and Samson, 1954; Swartzen-Allen and Matijevic, 1974; Williams and Williams, 1977; Zhao *et al.*, 2008), others refute them. Several researchers claim that due to the aspect ratio of the platelet particles, the edge face surface area was insufficiently large to provide a sufficient charge density to engender heterocoagulation with the basal face surface (Callaghan and Ottewill, 1974; Lagaly, 1989; Tateyama *et al.*, 1997). Instead, it is claimed that the predominant model of particle–particle interaction is that of FF coagulation.

Despite claims that the 'house of cards' or 'honeycomb' EF and EE particle arrangements are unlikely, their existence has been well demonstrated by the use of cryo-SEM techniques (Du *et al.*, 2010; McFarlane *et al.*, 2006). The source of the disagreement may lay in the assumptions with regards to the shape and aspect ratio of clay particles. A number of researchers assume a perfect thin-plate shape when making predictions about clay particle behaviour (Johnson *et al.*, 1998; Williams and Williams, 1977). However, studies have also clearly demonstrated that phyllosilicate particles do not often occur as thin, perfect flakes, but rather as poorly ordered structures, with sub-hedral facets and islands, resulting in a much higher proportion of edge surfaces being present (Żbik *et al.*, 2008, 2010).

Overall, different researchers have put forward a number of different potential mechanisms for predicting the particle–particle associations of clays in solution. In all likelihood,

there is no single correct way to describe such associations, and the overall clay behaviour is determined by a combination of all the described factors. To date, there is no firm understanding of the degree to which these different factors influence clay behaviour and how they vary with different clay types and clays from different sources.

2.6 Rheological Behaviour of Clay Suspensions

The rheology of a clay suspension, i.e. how it deforms in response to an applied stress, τ, has a significant effect on unit operations in mineral processing, such as pumping and pipeline transport, mixing and separation behaviour, and how tailings slurries behave on deposition in a tailings storage facility. Clay suspensions often behave in similar ways to other fine suspensions, as will be shown below, but their swelling behaviour in water makes them problematic for fluid-based mineral processing. The behaviour of viscous suspensions of clay in water will primarily be considered as these are most relevant to unit operations, water recovery, or disposal of waste streams (i.e. non-plastic systems). For clay as a semi-solid in a geotechnical context, see Murray (2006); for clay as a nano-composite filler in polymers, see Bhattacharya *et al.* (2008). A rudimentary knowledge of viscosity is assumed – otherwise, refer to Barnes *et al.* (1993).

2.6.1 Characterizing Suspensions

Viscosity at its most simple is a measure of a fluid's resistance to flow. For many rheologically complex materials the traditional definition of a fluid does not apply and an apparent viscosity is defined as the ratio between the applied shear stress and the resultant shear rate. The behaviour of the apparent viscosity as a function of shear rate is how a material is categorized rheologically. The broad characterization of time-independent, inelastic fluids that describe clay suspension is shown in the rheogram in Fig. 2.8. Newtonian behaviour is constant viscosity (at constant temperature) and is typical of simple fluids such as water, light hydrocarbons, and some low-concentration suspensions. Pseudoplastic behaviour can be described as 'shear thinning' with an apparent viscosity that decreases with increasing shear rate. This is seen in many aqueous polymers and molten thermoplastics. A yield pseudoplastic is also shear thinning but includes a yield stress, that is, a minimum applied shear stress that must be exceeded before flow commences. This is the most common behaviour observed for suspensions, including clay suspensions, and will be further discussed below. Shear thickening behaviour is an increase in the apparent viscosity with increasing shear rate. It was formerly known as 'dilatancy' but has been re-titled to distinguish it from volume dilatancy, which may occur simultaneously. Shear thickening occurs only in moderately to highly concentrated multi-phase mixtures, which are usually observed to have a yield stress as well (as is shown in Fig. 2.8). Shear thickening does not occur in typical clay suspensions, but the presence of an additional coarse solid phase at high enough concentration may produce this effect. Pseudoplastic, yield pseudoplastic and shear thickening behaviour are grouped as non-Newtonian material behaviours.

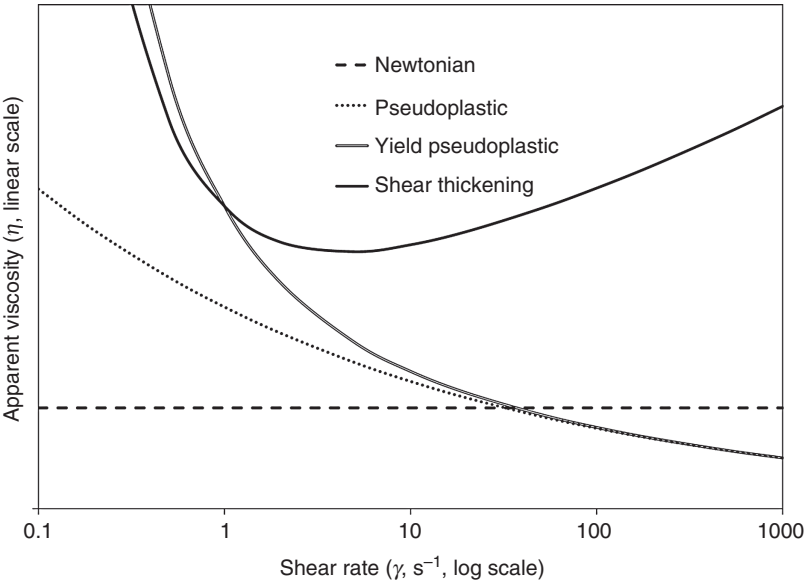

Figure 2.8. Representation of typical rheological behaviour of suspensions.

Suspension viscosity may also show time of shear dependency. If viscosity decreases with time at a constant shear stress or shear rate, and the effect is reversible by ceasing shear, then it is classified as thixotropic behaviour (see Fig. 2.9). If the reverse occurs it is anti-thixotropy (in earlier literature this was referred to as rheopexy). These terms are often confused with shear thinning or thickening, which are time independent, or rheomalaxis, which is the irreversible viscosity decrease with time. Thixotropic behaviour occurs in some more concentrated clay suspensions and mixtures; a well-studied industrial example is 'red mud' from bauxite processing (Nguyen and Boger, 1987). Thixotropic effects may occur due to shearing as a consequence of mixing, pumping or pipeline transport.

2.6.2 Factors Influencing Suspension Rheology

The rheological response of a suspension is a result of particle–fluid and particle–particle interactions. Suspension rheology can also be roughly categorized as resulting from mainly hydrodynamic forces or mainly from the influence of surface forces; this can vary with shear rate for a given suspension. Yield pseudoplastic behaviour can arise from both types of interaction, but usually begins at lower solids concentrations for suspensions with strong surface forces. The rheology of a suspension is therefore strongly dependant on the viscosity of the suspending medium and the inter-particle forces (see Section 2.4). The presence of electric double layers produces effects on the flow of the suspending medium that are referred to as electroviscous effects. The primary electroviscous effect is an increase in viscosity due to distortion of the electric double layer adding to energy dissipation from

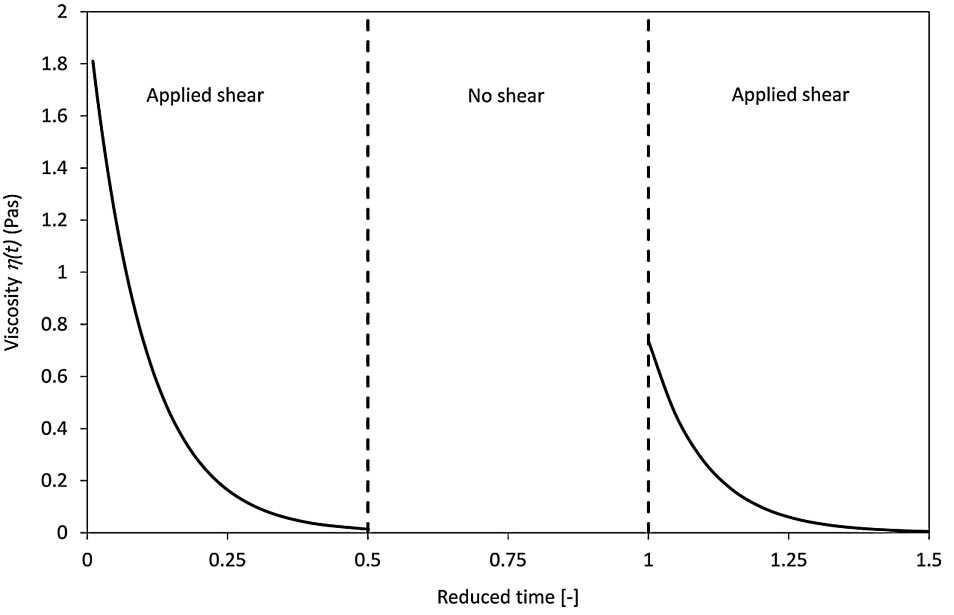

Figure 2.9. Thixotropic behaviour showing viscosity reduction during shearing, partial structure rebuild during rest and continued viscosity reduction with reapplication of shear.

the flow of the suspending medium. Secondary electroviscous effect is due to repulsion between double layers and the tertiary viscous effect includes all other inter- and intra-particle interactions that alter the geometry of the suspended medium. The suspending medium for the majority of the clay suspensions of interest is water, its viscosity showing only minor changes from varying salt content, but decreasing with increasing temperature. The number of interactions increase with concentration of the suspended phase, a dilute suspension having close to Newtonian behaviour (viscosity invariant with rate of shearing, $\dot{\gamma}$) and a higher concentration developing non-Newtonian effects (viscosity varying with shear rate and shear history). Types of non-Newtonian rheology displayed by clay suspensions are shown in Fig. 2.8.

Although it is not possible to predict a suspension's rheology a priori, a useful guide to how it will vary can be gained from the available semi-empirical models. The dimensional requirements of a model of suspension rheology are given by Stickel and Powell (2005), and they consider suspension viscosity η to be a function of particle and suspending medium properties:

$$\eta = f\left(a, \rho_p, \rho_n, \eta_m, \rho_f, kT, \dot{\gamma}.or.\tau, t\right) \tag{2.7}$$

where a is particle radius, ρ_p is particle density, ρ_n is particle number density, η_m is suspending medium viscosity, ρ_f is fluid density and kT is thermal energy. It should be noted that even this function is not exhaustive as a assumes a single particle size, not a size

distribution, and does not consider particle morphology, both of which have significant effects on rheological behaviour. These variables can be formed into six dimensionless groups:

$$\eta_r = f\left(C_v, \rho_r, N_{Pe}, N_{Re\dot{\gamma}}, t_r\right) \tag{2.8}$$

where $\eta_r = \eta / \eta_m$ (relative viscosity), $C_v = 4\pi\rho_n a^3/3$ (volume fraction), $\rho_r = \rho_p / \rho_f$ (reduced density), $N_{Pe} = 6\pi\eta a^3\dot{\gamma}/kT$ (Peclet number), $N_{Re\dot{\gamma}} = \rho_f a^2\dot{\gamma}/\eta$ (sheared particle Reynolds number) and $t_r = tkT/\eta a^3$ (reduced time).

For the special condition of a neutrally buoyant system, ρ_r can be ignored, and similarly at steady-state t_r may be neglected, leaving:

$$\eta_r = f\left(C_v, N_{Pe}, N_{Re\dot{\gamma}}\right) \tag{2.9}$$

Under conditions where $1/N_{Pe} \rightarrow 0$ and the Schmidt number ($N_{Sc} = N_{Pe} / N_{Re}$, a measure of shear-driven particle diffusivity) is large the suspension is likely to be Newtonian. This is the case when C_v is low and consequently suspension viscosity is a function of C_v only. This was derived theoretically by Einstein (1956):

$$\eta_r = 1 + C_v[\eta] \tag{2.10}$$

where $[\eta] = \lim_{C_v \to 0}\left(\frac{\eta_r - 1}{C_v}\right)$, the intrinsic viscosity which is largely a function of shape, with a value of 2.5 for hard spheres. The equation is effective for $C_v < 0.1$ and was improved upon by Batchelor (1977):

$$\eta_r = 1 + C_v[\eta] + k[\eta]^2 \tag{2.11}$$

where k is a function of suspension type, and has a value of 6.2 for Brownian suspensions. The parameter variations are due to changes in the primary electroviscous effects. A better approximation is obtained by including the maximum packing fraction C_{vm}, the geometrically highest achievable concentration where:

$$\lim_{C_v \to C_{vm}} \eta_r = \infty \tag{2.12}$$

C_{vm} is strongly dependant on particle size distribution and increases with polydispersity (Farris, 1968). One such model employing a reduced volume fraction is that of Krieger and Dougherty (1959):

$$\eta_r = \left(1 - \frac{C_v}{C_{vm}}\right)^{-[\eta]C_{vm}} \tag{2.13}$$

A comparison of these models is shown in Fig. 2.10. An extension to this model was introduced by Clarke (1967). By changing [η] values to reflect particle shape, non-spherical particles could be modelled; for a constant concentration, spheres yielded the

lowest viscosity, followed by plates. The highest viscosity was for rods or high-aspect-ratio objects. These three models all show the necessary increase in viscosity with increasing concentration but do not capture the non-Newtonian variation of viscosity with shear rate. This can be incorporated by using the technique of Wildemuth and Williams (1984, 1985) that was developed to describe the shear thinning behaviour of colloidal spheres and irregularly shaped coal suspensions (<100 μm; both are flocculating suspensions). This method considers that the maximum packing fraction C_{vm} is a function of shear stress:

$$\frac{1}{C_{vm}} = \frac{1}{C_{vm0}} - \left(\frac{1}{C_{vm0}} - \frac{1}{C_{vm\infty}} \right) \cdot C_{vd} \tag{2.14}$$

where C_{vm0} is a minimum value of packing fraction (at zero stress), $C_{vm\infty}$ is the highest value of packing fraction and C_{vd} is the fraction of particles that remain unflocculated and is related to the shear stress by:

$$C_{vd} = \frac{1}{1 + A\tau^{-m}} \tag{2.15}$$

where A and m are fitted parameters. A useful aspect of the Wildemuth and Williams method is that a yield stress, τ_y, is predicted for the condition $C_v < C_{vm}(\tau)$. As the imposed shear stress on a suspension decreases, so too does $C_{vm}(\tau)$ (from Eqs (2.14) and (2.15) until it is less than C_v). The yield stress will be discussed further below. Meaning can be assigned to the various parameters in Eqs (2.14) and (2.15) in terms of strength and type of interaction; however, they are still largely experimentally derived or fitted values and cannot be estimated from knowledge of suspended phase conditions. As concentration of the dispersed phase increases, the multiple body interactions increase rapidly and make prediction of bulk properties overly complex.

Useful models of the rheological behaviour of suspensions have been developed for describing the transport properties of suspensions such as clay in water. Most models suitable for yield pseudoplastics are mathematical fits with limited physical meaning in their parameters. The Herschel–Bulkley model (see Eqs (2.16) and (2.17)) is one such instance (Coussot *et al*., 1996; Pignon *et al.*, 1997):

$$\tau = \tau_y + k\dot{\gamma}^n \tag{2.16}$$

$$\eta = \frac{\tau_y}{\dot{\gamma}} + \dot{\gamma}^{(n-1)} \tag{2.17}$$

where k is a measure of the consistency of the fluid; and n the flow behaviour index. Real, non-dilute clay suspensions cannot be described effectively by simple two-parameter models such as the power-law equation, Bingham plastic equation or Casson equation (Casson, 1959). This is because the structures and interactions that give rise to shear thinning will also give rise to yield stresses. The Herschel–Bulkley model imperfectly captures the viscosity behaviour of many suspensions, but is adequate over a limited range of shear rates.

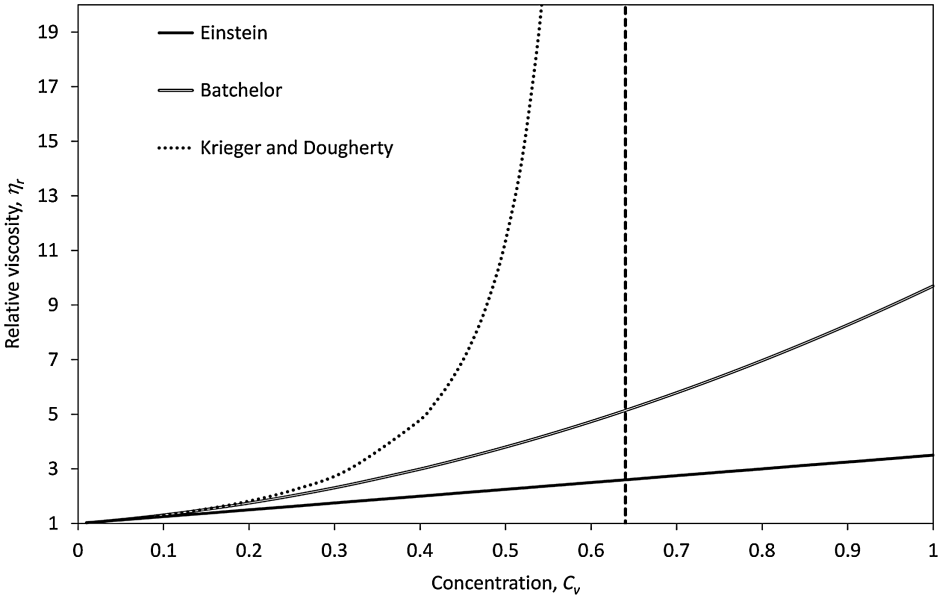

Figure 2.10. Three models of relative viscosity for suspensions.

The yield stress has been mentioned already, but its role in suspension rheology requires some further discussion. A yield stress can arise in a suspension of interacting or non-interacting particles, but will be seen more readily at lower concentrations when strong surface forces are present. This is typically the case for clay-based slurries. Due to the relative ease of taking repeatable yield stress measurements compared to more complete shear stress rheograms (see Section 2.6.3) and the strong dependence on network structures, the yield stress is a common means of monitoring changes in clay suspension behaviour. There are a limited number of studies that attempt to relate the physical properties of particles to the yield stress response of suspensions (e.g. Gay *et al.*, 1969; Thomas, 1961) without incorporating the mechanisms responsible. The effects of surface chemistry on rheology, such as van der Waals and electrical double-layer forces, has been related to the yield stress of suspensions of spheres by Scales *et al.* (1998). The yield stress is found to be a strong function of the zeta potential, and at a maximum when the zeta potential is zero (i.e. at the iso-electric point). The relationship is more complicated in mineral suspensions and does not simply rely on a single parameter (Franks *et al.*, 1999). In the studies cited above, where suspensions are colloidal and inter-particle forces are significant, the yield stress is often related to the breaking of bonds or the breaking up of agglomerates. Experimentally the presence of a static yield stress in dense suspensions is familiar to those working with them regularly and their existence has been established convincingly by Husband *et al.* (1993) and by Huang *et al.* (2005), among others.

2.6.3 Rheometry

Measurement of rheological properties (rheometry) is the characterization of changes to the momentum transport properties of a material. Modelling rheological data is useful for engineering design in pipelines, mixing and thickening. Rheology can also be used as a surrogate for other less readily testable phenomena due to the relative ease of testing bulk properties in place of phenomena at the scale of particle dimensions. Rheometry, however, does not provide a priori insights into material structure as the measured property changes can arise from many causes. It is only a useful indicator once it has been 'calibrated' against the phenomena of interest by other, non-rheological, tests. Many of the studies cited in Section 2.6.4 are of this type.

As many of the clay suspensions of interest are non-Newtonian, a suitable rheometer needs to measure a range of defined shear rates and shear stresses for a given sample. Older types of viscometer, such as the ubiquitous Brookfield, Fann or Hercules, do not measure true rheology as they lack a defined shear field. Important distinctions between sample behaviour are therefore missed. Rotational rheometers using cone and plate, parallel plate or Couette geometries are suitable for clay–water suspensions (Whorlow, 1980), but the cone and plate geometries are not suitable if larger particles or structures are present. Pressure-driven capillary instruments are useful for higher shear rates if the non-Newtonian effects are allowed for in the interpretation of the data using the Rabinowitsch–Mooney equation (Barnes *et al.*, 1993). Apart from unidirectional rotational rheometry, it is possible to apply oscillatory shear to deform a sample without causing unrecoverable strain or disrupting any possible network structure. This technique is not useful for determining transport properties, but may provide some insight into the condition of particle arrangement, notwithstanding the caveat regarding a priori insights from rheometry.

Thixotropy is often detected in concentrated clay suspensions and can manifest as a hysteresis loop on a rheogram. Although commonly taken as a means of comparison between samples (e.g. Brandenburg and Lagaly, 1988; Christidis *et al.*, 2006), a hysteresis loop is actually not a fundamental property but rather an artefact of how the test is conducted. Thixotropic behaviour is best characterized at constant shear rate (or shear stress) and the decay in viscosity recorded as in Fig. 2.9. This allows for analysis using simpler models of $\eta(t)$.

Rheometry is further complicated by experimental artefacts such as wall slippage, which occurs when the suspension being sheared moves relative to the surfaces of the measurement geometry. Slip is more likely to occur and increase in severity as concentration of the dispersed phase increases. It is possible to minimize (but not eliminate) wall slip through the roughening or profiling of measurement surfaces, although it is preferable to use one of many available techniques to de-convolute the rheological and slip behaviour of a suspension (see Chryss *et al.*, 2005 or Mooney, 1931). These techniques involve tests in multiple measuring geometries of different dimensions and consequently increase the number of tests required per sample. Unsurprisingly, the majority of experimental data presented for shear rheometry of clay suspensions, or suspensions generally, are not proofed against slip

effects. A simple work-around to avoid slip artefacts is to use a vane rheometer to provide a value of the yield stress (Nguyen and Boger, 1987). This is a highly repeatable technique that provides valuable data for comparison between samples and an indication of a materials slump characteristics (see Schowalter and Christensen, 1998). The main drawback to the vane method is that it only provides data at a single point, i.e. at a zero shear rate. Several of the studies cited in Section 2.6.4 utilize this method.

2.6.4 Chemistry Changes and Rheology

The rheology of clay–water suspensions has been studied extensively in relation to the ceramics industry (Worrall, 1986) and to drilling muds for petroleum extraction (Kassab *et al.*, 2011). Consequently, bentonite and kaolinite tend to dominate the literature. The effect of pH, electrolyte concentration and Na:Ca:Mg ratio on rheology, in particular yield stress, has been widely reported. A maximum in the yield stress of bentonite at its 'natural' (i.e. acidic) pH is reported by Kelessidis *et al.* (2007), Benna *et al.* (1999) and Brandenburg and Lagaly (1988). Similar results were reported for sepiolite (Çınar *et al.*, 2009), but with a basic natural pH. Attapulgite is largely unaffected by pH or NaCl content (Chang *et al.*, 1993), hence its efficacy as a drilling fluid in salty conditions. Yong and Ohtsubo (1987) observed that kaolinite has a monotonically decreasing yield stress with pH, but the addition of iron hydroxide as ferrihydrate can produce maxima similar to those of bentonites.

The effect of NaCl concentration on bentonite has been covered by many workers, with similar outcomes. Abend and Lagaly (2000) found small minima in rheological properties at low NaCl content. They also found similar minima with other chlorides and with Na_2SO_4. Penner and Lagaly (2001) found viscosity minima for chloride and nitrate salt addition, again at low concentration (~1 mmol). De Kretser *et al.* (1998) found a large maximum in yield stress with NaCl content at concentrations two orders of magnitude higher. Güler and Balci (1998) saw an increase in viscosity for kaolinitic clays with the addition of salts, the effect being stronger for chlorides over sulphides and no minima were present. Alther (1986) determined a strong correlation between the ratios of exchangeable cations in bentonite and the viscosity of a clay suspension.

Brandenburg and Lagaly (1988) state that the dependence of flow behaviour on salt concentration and pH can be explained by different types of particle aggregation. Similarly, de Kretser *et al.* (1998), in examining thixotropic behaviour in sodium-montmorillonite-based suspensions, explains the effect of higher NaCl concentrations as due to FF aggregation, which reduces the number of interacting flow units and consequently the rheological parameters such as yield stress.

Clay rheology deviates from simple concentration dependency such as Eq. (2.10) due to particle anisotropy (Packter, 1962). Yuan and Murray (1997) tested the viscosity of high-solids kaolin suspensions with differing particle morphology. The lowest viscosity was shown by a spherical halloysite, a platy kaolinite was higher and a tubular halloysite was highest. This corresponds to the modelling of suspensions of differing shaped particles by Clarke (1967).

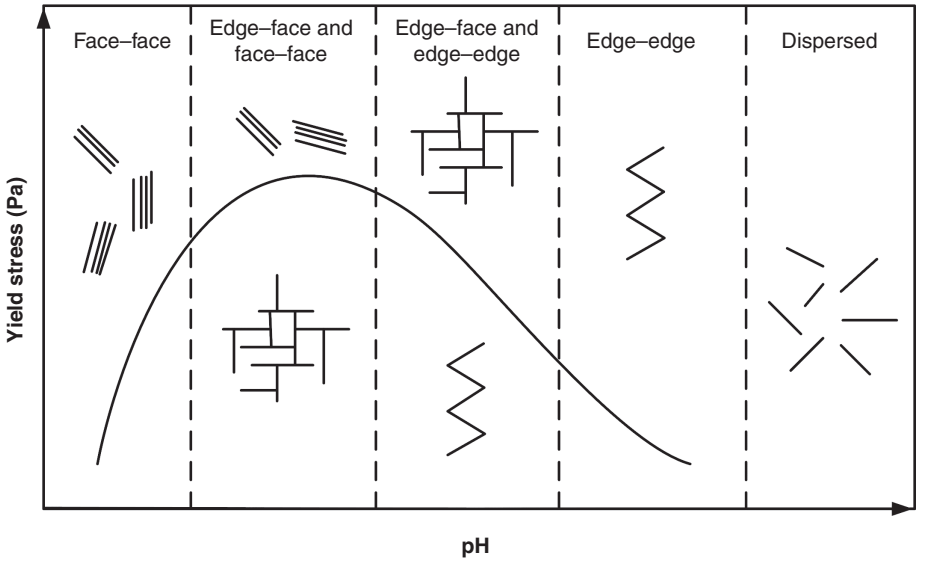

Figure 2.11. Schematic representation of rheological behaviour resulting from different particle orientations (based on observed Bingham yield values; Rand and Melton, 1976).

2.6.5 Effect of Particle Orientation on Suspension Rheology

The different orientations of the clay particles can directly influence the rheological behaviour of mineral suspension through factors like effective volume fraction and the presence of strong inter-particle forces (both attractive and repulsive).

The effect of particle orientations on suspension yield stress was first proposed by Rand and Melton (1976), as described in Fig. 2.11. It must be noted that in their interpretation Rand and Melton focus on lower pH regions and have left out the mention of FF coagulation. Figure 2.11 was adapted from the original publication and altered to reflect the presence of FF coagulation in the acidic pH region.

Rand and Melton postulate that at high pH values, particles will be completely dispersed, thus resulting in low (or zero) Bingham yield stresses. As the pH decreases, the particles begin to aggregate into different particle–particle orientation, described in the previous section.

At relatively high pH values, the predominant orientation is thought to be that of EE, forming loosely bonded, open structures. This causes an elevation in the yield stress of the suspension. As the pH decreases further, the charge on the particle edges approaches neutrality, and EF (house of cards) structures begin to form. Such open structures are thought to be bonded by strong heterocoagulation forces and trap water within them. A combination of these two factors is thought to further increase the suspension yield stress.

As the pH continues to decrease, the predominant orientation becomes that of EF structures. However more compact FF aggregates also begin to form. FF aggregates have a lower

effective volume than EF aggregates, which halts the continuous increase in the suspension yield stress, resulting in maximum peak. A further decrease in suspension pH results in FF aggregates becoming dominant, driving the suspension yield stress further down.

It is important to stress that the particle coordination/rheology relationship described in Fig. 2.11 is highly generalized and speculative. It can be further modified by including the effect of electrolytes (Lagaly and Ziesmer, 2003), which will alter the type of coordination that occurs at a given pH, and consequently the rheology. The yield stress/pH relationship for anisotropic clays generally adheres to the shape of the described curve (i.e. exhibits a peak), but neither the location of the peak with regards to the pH, nor the magnitude of the peak can be predicted with any degree of accuracy for a specific mineral under a specified set of chemical conditions.

2.7 Summary

Overall, the lack of agreement as to the exact nature of the mechanisms that drive the interparticle interactions of phyllosilicate suspensions only serves to emphasize the complexity of the process. As a result, there is no fundamental or mechanistic model in existence that adequately describes or predicts the behaviour of clay minerals in suspension. Some authors have even claimed that DLVO theory as a whole is not sufficient to describe and predict colloidal stability of anisotropic clay particles (Missana and Adell, 2000). This assertion is based on the persistent incongruity between model predictions and experimental results.

However, these inconsistencies appear to be based on inadequate assumptions and estimates of the mineral properties that act as input parameters into the DLVO equations (such as Hamaker constants and surface potential values), rather than the theory itself. Hopefully, the latest developments in cryo-SEM, AFM and X-ray diffraction techniques will pave the way for future work that will finally elucidate consistent mechanisms for clay particle interactions and allow for the development of accurate predictive models.

Similarly, rheology suspension theory rapidly fails as moderate concentrations are examined. Prediction of rheological properties is difficult due to the confounding of multiple factors; a combination of particle–particle and fluid–particle interactions (which are affected by pH and electrolyte type and strength) with the particle morphology and size distribution produce rheological behaviour that is not possible to predict well from non-rheological measurements. This does not mean that understanding the rheology of clay suspensions is not useful. When appropriate measurement techniques are applied information that leads to engineering prediction and design can be derived, and means to rheology modification are indicated.

References

Abend, S. & Lagaly, G. 2000. Sol–gel transitions of sodium montmorillonite dispersions. *Applied Clay Science*, 16 (3–4), 201–227.

Adamson, A. W. 1985. *Physical Chemistry of Surfaces*. New York: Wiley & Sons.

Alther, G. R. 1986. The effect of the exchangeable cations on the physico-chemical properties of Wyoming bentonites. *Applied Clay Science*, 1 (3), 273–284.
Arnold, B. J. & Aplan, F. F. 1986. The effect of clay slimes on coal flotation, part I: The nature of the clay. *International Journal of Mineral Processing*, 17 (3–4), 225–242.
Attia, Y. A. & Deason, D. M. 1989. Control of slimes coating in mineral suspensions. *Colloids and Surfaces*, 39 (1), 227–238.
Barnes, H. A., Hutton, J. F. & Walters, K. 1993. *An Introduction to Rheology*. Amsterdam: Elsevier.
Batchelor, G. K. 1977. The effect of Brownian motion on the bulk stress in a suspension of spherical particles. *Journal of Fluid Mechanics*, 83 (1), 97–117.
Benna, M., Kbir-Ariguib, N., Magnin, A. & Bergaya, F. 1999. Effect of pH on rheological properties of purified sodium bentonite suspensions. *Journal of Colloid and Interface Science*, 218 (2), 442–455.
Bhattacharya, S. N., Kamal, M. R. & Gupta, R. K. 2008. *Polymeric Nanocomposites: Theory and Practice*. Berlin: Hanser Publishers.
Bracke, G., Satir, M. & Krauss, P. 1995. The cryptand [222] for exchanging cations of micas. *Clays and Clay Minerals*, 43 (6), 732–737.
Brandenburg, U. & Lagaly, G. 1988. Rheological properties of sodium montmorillonite dispersions. *Applied Clay Science*, 3 (3), 263–279.
Bremmell, K. E. & Addai-Mensah, J. 2005. Interfacial chemistry mediated behaviour of colloidal talc dispersions. *Journal of Colloid and Interface Science*, 283, 385–391.
Burdukova, E., Bradshaw, D. J. & Laskowski, J. S. 2007. Effect of CMC and pH on the rheology of suspensions of isotropic and anisotropic minerals. *Canadian Metallurgical Quarterly*, 46, 273–278.
Burdukova, E., Becker, M., Ndlovu, B., Mokgethi, B. & Deglon, D. A. 2008. Relationship between slurry rheology and its mineralogical content. In: Wang, D. D., Xao, S. C., Wang, F. L., Cheng, Z. U. & Long, H., (eds) *24th Int. Minerals Processing Congress*. Beijing: China Scientific Book Service Co. Ltd, 2169–2178.
Callaghan, I. C. & Ottewill, R. H. 1974. Interparticle forces in montmorillonite gels. *Faraday Discussions of the Chemical Society*, 57, 110–118.
Casson, N. 1959. A flow equation for pigment-oil suspensions of the printing ink type. In: Mill, C. C. (ed.) *Rheology of Disperse Systems.* London: Pergamon Press.
Chang, S. H., Ryan, M. H. & Gupta, R. K. 1993. The effect of pH, ionic strength, and temperature on the rheology and stability of aqueous clay suspensions. *Rheologica Acta*, 32 (3), 263–269.
Christidis, G. E., Blum, A. E. & Eberl, D. D. 2006. Influence of layer charge and charge distribution of smectites on the flow behaviour and swelling of bentonites. *Applied Clay Science*, 34 (1–4), 125–138.
Chryss, A., Bhattacharya, S. & Pullum, L. 2005. Rheology of shear thickening suspensions and the effects of wall slip in torsional flow. *Rheologica Acta*, 45 (2), 124–131.
Churchman, G. J. 1980. Clay minerals from micas and chlorites in some New Zealand soils. *Clay Minerals*, 15, 59–76.
Çınar, M., Can, M. F., Sabah, E., Karagüzel, C. & Çelik, M. S. 2009. Rheological properties of sepiolite ground in acid and alkaline media. *Applied Clay Science*, 42 (3–4), 422–426.
Clarke, B. 1967. Rheology of coarse settling suspensions. *Transactions of the Institution of Chemical Engineers*, 45, 251–256.
Coussot, P., Proust, S. & Ancey, C. 1996. Rheological interpretation of deposits of yield stress fluids. *Journal of Non-Newtonian Fluid Mechanics*, 66(1), 55–70.

Craig, V. S. J., Ninham, B. W. & Pashley, R. M. 1998. Study of the long-range hydrophobic attraction in concentrated salt solutions and its implications for electrostatic models. *Langmuir*, 14 (12), 3326–3332.

Craig, V. S. J., Ninham, B. W. & Pashley, R. M. 1999. Direct measurement of hydrophobic forces: A study of dissolved gas, approach rate, and neutron irradiation. *Langmuir*, 15 (4), 1562–1569.

de Kretser, R., Scales, P. J. & Boger, D. V. 1997. Improving clay-based tailings disposal: Case study on coal tailings. *American Institute of Chemical Engineers Journal*, 43 (7), 1894–1903.

de Kretser, R. G., Scales, P. J. & Boger, D. V. 1998. Surface chemistry–rheology interrelationships in clay suspensions. *Colloids and Surfaces A: Physicochemical and Engineering Aspects*, 137 (1), 307–318.

Deer, W. A., Howie, R. A. & Zussman, J. 1992. *Introduction to Rock-Forming Minerals*. New York: Prentice Hall.

Derjaguin, B. V. & Landau, L. 1941. Theory of stability of strongly charged lyophobic sols and the adhesion of strongly charged particles in solution of electrolytes. *Acta Physiochimica*, 14, 633–662.

Du, J., Morris, G., Pushkarova, R. A. & St. C. Smart, R. 2010. Effect of surface structure of kaolinite on aggregation, settling rate, and bed density. *Langmuir*, 26 (16), 13227–13235.

Duc, M., Gaboriaud, F. & Thomas, F. 2005a. Sensitivity of the acid–base properties of clays to the methods of preparation and measurement: 1. Literature review. *Journal of Colloid and Interface Science*, 289 (1), 139–147.

Duc, M., Gaboriaud, F. & Thomas, F. 2005b. Sensitivity of the acid–base properties of clays to the methods of preparation and measurement: 2. Evidence from continuous potentiometric titrations. *Journal of Colloid and Interface Science*, 289 (1), 148–156.

Dukhin, S. S. & Derjaguin, B. V. 1976. *Electrophoresis*. Moscow: Academy of Sciences of the USSR.

Einstein, A. 1956. *Investigations on the Theory of the Brownian Movement*. Mineola, NY: Dover Publications, Inc.

Farris, R. J. 1968. Prediction of the viscosity of multimodal suspensions from unimodal viscosity data. *Transactions of the Society of Rheology*, 12 (2), 281–302.

Franks, G. V., Johnson, S. B., Scales, P. J., Boger, D. V. & Healy, T. W. 1999. Ion-specific strength of attractive particle networks. *Langmuir*, 15 (13), 4411–4420.

Fuerstenau, D. W. & Huang, P. 2003. Interfacial phenomena involved in talc flotation. In: D. J. Bradshaw (ed.) *22nd Int. Minerals Processing Congress*. Cape Town: Document Transformation Technologies, 1034–1043.

Fuerstenau, D. W., Gaudin, A. M. & Miaw, H. L. 1958. Iron oxide slime coatings in flotation. *Transactions of the American Institute of Mining, Metallurgy, and Petroleum Engineers*, 211, 792–793.

Fuerstenau, M. C., Valdivieso, A. & Fuerstenau, D. W. 1988. Role of hydrolyzed cations in the natural hydrophobicity of talc. *International Journal of Minerals Processing*, 23, 161–170.

Gay, E. C., Nelson, P. A. & Armstrong, W. P. 1969. Flow properties of suspensions with high solids concentration. *AIChE Journal*, 15 (6), 815–822.

Gregory, J. 2006. *Particles in Water, Properties and Processes*. Boca Raton, FL: Taylor & Francis.

Güler, Ç. & Balci, E. 1998. Effect of some salts on the viscosity of slip casting. *Applied Clay Science*, 13 (3), 213–218.

Hiemenz, P. C. & Rajagopolan, R. 1997. *Principles of Colloid Chemistry.* New York: Dekker.
Hogg, R., Healy, T. W. & Fuerstenau, D. W. 1966. Mutual coagulation of colloidal dispersions. *Transactions of the Faraday Society*, 62, 1638–1651.
Hou, J., Li, H., Zhu, H. & Wu, L. 2009. Determination of clay surface potential: A more reliable approach. *Soil Science Society of America Journal*, 73 (5), 1658–1663.
Huang, N., Ovarlez, G., Bertrand, F., *et al.* 2005. Flow of wet granular materials. *Physical Review Letters*, 94 (2), 028301.
Hunter, R. J. 1988. *Zeta Potential in Colloid Science: Principles and Applications.* San Diego, CA: Academic Press.
Husband, D. M., Aksel, N. & Gleissle, W. 1993. The existence of static yield stresses in suspensions containing noncolloidal particles. *Journal of Rheology*, 37 (2), 215–235.
Ishida, N., Sakamoto, M., Miyahara, M. & Higashitani, K. 2000a. Attraction between hydrophobic surfaces with and without gas phase. *Langmuir*, 16, 5681–5687.
Ishida, N., Inoue, T., Miyahara, M. & Higashitani, K. 2000b. Nano bubbles in a hydrophobic surface in water observed by tapping-mode atomic force microscopy. *Langmuir*, 16, 6377–6380.
Israelachvili, J. 1985. *Intermolecular & Surface Forces*. London: Academic Press.
Israelachvili, J. N. & Pashley, R. M. 1983. Measurement of the hydrophobic interaction between two hydrophobic surfaces in aqueous electrolyte solution. *Journal of Colloid and Interface Science*, 98 (2), 500–514.
Iwasaki, I., Cooke, S. R. B., Haraway, D. H. & Choi, H. S. 1962. Iron wash slimes: Some mineralogical characteristics. *Transactions AIME*, 223, 97–108.
Janek, M. & Lagaly, G. 2001. Proton saturation and rheological properties of smectite dispersions. *Applied Clay Science*, 19 (1–6), 121–130.
Johnson, S. B., Russell, A. S. & Scales, P. J. 1998. Volume fraction effects in shear rheology and electroacoustic studies of concentrated alumina and kaolin suspensions. *Colloids and Surfaces*, 141, 119–130.
Kassab, S. Z., Ismail, A. S. & Elessawi, M. M. 2011. Drilling fluid rheology and hydraulics for oil fields. *European Journal of Scientific Research*, 57 (1), 68–86.
Kelessidis, V. C., Tsamantaki, C. & Dalamarinis, P. 2007. Effect of pH and electrolyte on the rheology of aqueous Wyoming bentonite dispersions. *Applied Clay Science*, 38 (1–2), 86–96.
Kitchener, J. A. 1969. Colloid minerals: Chemical aspects of their dispersion, flocculation and filtration. *Filtration and Separation*, 6 (5), 553–558.
Klein, C. & Hurlbut, C. S. 1993. *Manual of Mineralogy.* New York: Wiley & Sons.
Krieger, I. M. & Dougherty, T. J. 1959. A mechanism for non-Newtonian flow in suspensions of rigid spheres. *Transactions of the Society of Rheology*, 3 (1), 137–152.
Kurihara, K., Kato, S. & Kunitake, T. 1990. Very strong long range attractive forces between stable hydrophobic monolayers of a polymerized ammonium surfactant. *Chemistry Letters*, 19 (9), 1555.
Lagaly, G. 1989. Principles of flow of kaolin and bentonite dispersions. *Applied Clay Science*, 4 (2), 105–123.
Lagaly, G. & Ziesmer, S. 2003. Colloid chemistry of clay minerals: The coagulation of montmorillonite dispersions. *Advances in Colloid and Interface Science*, 100–102, 105–128.
Laskowski, J. S. & Pugh, R. J. 1992. Dispersion stability and dispersing agents. In: Laskowski, J. S. & Ralston, J. (eds) *Colloid Chemistry in Mineral Processing.* New York: Elsevier.

Laskowski, J. S. & Sobieraj, S. 1969. Zero points of charge of spinel minerals. *Transactions of the Canadian Institute of Mining and Metallurgy*, 78, C161–C162.
Liu, J., Zhou, Z., Xu, Z. & Masliyah, J. 2002. Bitumen–clay interactions in aqueous media studied by zeta potential distribution measurement. *Journal of Colloid and Interface Science*, 252 (2), 409–418.
Luckham, P. S. & Rossi, S. 1999. The colloidal and rheological properties of bentonite suspensions. *Journal of Colloid and Interface Science*, 82, 43–92.
Mantel, M., Rabinovich, Y. I., Wightman, J. P. & Yoon, R. H. 1995. A study of hydrophobic interactions between stainless steel and salinated glass surfaces using atomic force microscopy. *Journal of Colloid and Interface Science*, 170, 203–214.
Marra, J. & Hair, M. L. 1988. Forces between two poly(2-vinylpyridine)-covered surfaces as a function of ionic strength and polymer charge. *The Journal of Physical Chemistry*, 92 (21), 6044–6051.
McFarlane, A., Bremmell, K. & Addai-Mensah, J. 2005. Microstructure, rheology and dewatering behaviour of smectite dispersions during orthokinetic flocculation. *Minerals Engineering*, 18 (12), 1173–1182.
McFarlane, A., Bremmell, K. & Addai-Mensah, J. 2006. Improved dewatering behavior of clay minerals dispersions via interfacial chemistry and particle interactions optimization. *Journal of Colloid and Interface Science*, 293 (1), 116–127.
Meagher, L. & Craig, V. S. J. 1994. Effect of dissolved gas and salt on the hydrophobic force between polypropylene surfaces. *Langmuir*, 10 (8), 2736–2742.
Mellini, M. & Zanazzi, P. R. 1987. Crystal structures of lizardite-IT and lizardite-2Hl from Coli, Italy. *American Mineralogist*, 72, 941–948.
Meyer, E. E., Rosenberg, K. J. & Israelachvili, J. 2006. Recent progress in understanding hydrophobic interactions. *Proceedings of the National Academy of Sciences of United States of America*, 103 (43), 15739–15746.
Missana, T. & Adell, A. 2000. On the applicability of DLVO theory to the prediction of clay colloids stability. *Journal of Colloid and Interface Science*, 230 (1), 150–156.
Mooney, M. 1931. Explicit formulas for slip and fluidity. *Journal of Rheology*, 2 (2), 210–222.
Mular, A. L. & Roberts, R. B. 1966. A simplified method to determine isoelectric points of oxides. *Transactions of the Canadian Institute of Mining and Metallurgy*, 69, 438–439.
Murray, H. H. 2006. Exploration, mining, and processing. In: Haydn, H. M. (ed.) *Developments in Clay Science.* New York: Elsevier.
Nalaskowski, J., Abdul, B., Du, H. & Miller, J. D. 2007. Anisotropic character of talc surfaces as revealed by streaming potential measurements, atomic force microscopy, molecular dynamics simulations and contact angle measurements. *Canadian Metallurgical Quarterly*, 46 (3), 227–235.
Ndlovu, B. N., Forbes, E., Becker, M., *et al.* 2011. The effects of chrysotile mineralogical properties on the rheology of chrysotile suspensions. *Minerals Engineering*, 24 (9), 1004–1009.
Nguyen, Q. D. & Boger, D. V. 1987. The rheology of concentrated bauxite residue suspensions: a complete story. In: Wagh, A. S. & Desai, P. (eds) *Bauxite Tailings 'Red Mud'*. Kingston: The Jamaica Bauxite Institute.
Nishimura, S., Scales, P. J., Tateyama, H., Tsunematsu, K. & Healy, T. W. 1995. Cationic modification of muscovite mica: An electrokinetic study. *Langmuir*, 11 (1), 291–295.
Packter, A. 1962. Studies in the rheology of clay–water systems. *Rheologica Acta*, 2 (1), 44–50.

Pashley, R. M., McGuiggan, P. M. & Ninham, B. W. 1985. Attractive forces between uncharged hydrophobic surfaces: Direct measurement in aqueous solution. *Science*, 229, 1088–1089.

Penner, D. & Lagaly, G. 2001. Influence of anions on the rheological properties of clay mineral dispersions. *Applied Clay Science*, 19 (1–6), 131–142.

Pignon, F., Magnin, A., Piau, J.-M., *et al.* 1997. Yield stress thixotropic clay suspension: Investigations of structure by light, neutron, and x-ray scattering. *Physical Review E*, 56 (3), 3281–3289.

Power, G., Gräfe, M. & Klauber, C. 2011. Bauxite residue issues: I. Current management, disposal and storage practices. *Hydrometallurgy*, 108 (1–2), 33–45.

Rabinovich, Y. I. & Derjaguin, B. V. 1988. Interaction of hydrophobized filaments in aqueous electrolyte solutions. *Colloids and Surfaces*, 30 (3–4), 243–251.

Ralston, J. & Fornaserio, D. 2006. Effect of MgO minerals on pentlandite flotation. In: Onal, G., Acarkan, N., Celik, M. S., *et al.* (eds) *23rd International Minerals Processing Congress*. Istanbul:Promed Advertising Ltd, 750–755.

Rand, B. & Melton, I. E. 1975. Isoelectric point of edge surface of kaolinite. *Nature*, 257, 214–216.

Rand, B. & Melton, I. E. 1976. Particle interactions in aqueous kaolinite suspensions. *Journal of Colloid and Interface Science*, 60 (2), 308–320.

Scales, P. J., Grieser, F. & Healy, T. W. 1990. Electrokinetics of the muscovite mica–aqueous solution interface. *Langmuir*, 6 (3), 582–589.

Scales, P. J., Johnson, S. B., Healy, T. W. & Kapur, P. C. 1998. Shear yield stress of partially flocculated colloidal suspensions. *American Institute of Chemical Engineers Journal*, 44 (3), 538–544.

Schofield, R. K. & Samson, H. R. 1954. Flocculation of kaolinite due to the attraction of oppositely charged crystal faces. *Discussions of the Faraday Society*, 18, 135–145.

Schouwstra, R. P., Kinloch, E. D. & Lee, C. A. 2000. A short geological review of the Bushvelt Complex. *Platinum Metals Review*, 44, 33–39.

Schowalter, W. R. & Christensen, G. 1998. Toward a rationalization of the slump test for fresh concrete: Comparisons of calculations and experiments. *Journal of Rheology*, 42 (4), 865–870.

Senior, G. D. & Thomas, S. A. 2005. Development and implementation of a new flowsheet for the flotation of a low grade nickel ore. *International Journal of Mineral Processing*, 78 (1), 49–61.

Sofrá, F. & Boger, D. V. 2002. Environmental rheology for waste minimisation in the minerals industry. *Chemical Engineering Journal*, 86 (3), 319–330.

Steenberg, E. & Harris, P. J. 1984. Adsorption of carboxymethyl cellulose, guar gum and starch onto talc, sulphides, oxides and salt type minerals. *South African Journal of Chemistry*, 37, 85–90.

Stickel, J. J. & Powell, R. L. 2005. Fluid mechanics and rheology of dense suspensions. *Annual Review of Fluid Mechanics.* 37, 129–149.

Swartzen-Allen, S. L. & Matijevic, E. 1974. Surface and colloid chemistry of clays. *Chemical Reviews*, 74 (3), 385–400.

Tateyama, H., Scales, P. J., Ooi, M., *et al.* 1997. X-ray diffraction and rheology study of highly ordered clay platelet alignment in aqueous solutions of sodium tripolyphosphate. *Langmuir*, 13 (9), 2440–2446.

Thomas, D. G. 1961. Transport characteristics of suspensions: 3. Laminar-flow properties of flocculated suspensions. *AIChE Journal*, 7 (3), 431–437.

Tombácz, E. & Szekeres, M. 2004. Colloidal behavior of aqueous montmorillonite suspensions: The specific role of pH in the presence of indifferent electrolytes. *Applied Clay Science*, 27 (1–2), 75–94.

Tombácz, E. & Szekeres, M. 2006. Surface charge heterogeneity of kaolinite in aqueous suspension in comparison with montmorillonite. *Applied Clay Science*, 34, 105–124.

van Olphen, H. 1951. Rheological phenomena of clay sols in connection with the charge distribution on the micelles. *Discussions of the Faraday Society*, 11, 83–96.

Verwey, E. J. W. & Overbeek, J. T. G. 1948. *Theory of Stability of Lyophobic Solids.* Amsterdam: Elsevier.

Whorlow, R. W. 1980. *Rheological Techniques*. Sussex: Ellis Horwood.

Wildemuth, C. R. & Williams, M. C. 1984. Viscosity of suspensions modeled with a shear-dependent maximum packing fraction. *Rheologica Acta*, 23 (6), 627–635.

Wildemuth, C. R. & Williams, M. C. 1985. A new interpretation of viscosity and yield stress in dense slurries: Coal and other irregular particles. *Rheologica Acta*, 24 (1), 75–91.

Williams, D. J. A. & Williams, K. P. 1977. Electrophoresis and zeta potential of kaolinite. *Journal of Colloid and Interface Science*, 65 (1), 79–87.

Worrall, D. M. 1986. *Clays and Ceramic Raw Materials*. Dordrecht: Springer.

Xu, Z., Liu, J., Choung, J. W. & Zhou, Z. 2003. Electrokinetic study of clay interactions with coal in flotation. *International Journal of Mineral Processing*, 68 (1–4), 183–196.

Yada, K. 1971. Study of microstructure of chrysotile asbestos by high resolution electron microscopy. *Acta Chrystallographica A*, A27 (6), 659–664.

Yan, L., Englert, A. H., Masliyah, J. H. & Xu, Z. 2011. Determination of anisotropic surface characteristics of different phyllosilicates by direct force measurements. *Langmuir*, 27 (21), 12996–13007.

Yin, X., Gupta, V., Du, H., Wang, X. & Miller, J. D. 2012. Surface charge and wetting characteristics of layered silicate minerals. *Advances in Colloid and Interface Science*, 179–182, 43–50.

Yong, R. N. & Ohtsubo, M. 1987. Interparticle action and rheology of kaolinite–amorphous iron hydroxide (ferrihydrite) complexes. *Applied Clay Science*, 2 (1), 63–81.

Yuan, J. & Murray, H. H. 1997. The importance of crystal morphology on the viscosity of concentrated suspensions of kaolins. *Applied Clay Science*, 12 (3), 209–219.

Żbik, M. S., Smart, R. S. C. & Morris, G. E. 2008. Kaolinite flocculation structure. *Journal of Colloid and Interface Science*, 328 (1), 73–80.

Żbik, M. S., Martens, W. N., Frost, R. L., *et al.* 2010. Smectite flocculation structure modified by Al13 macro-molecules – As revealed by the transmission X-ray microscopy (TXM). *Journal of Colloid and Interface Science*, 345 (1), 34–40.

Zhang, X. H., Quinn, A. & Ducker, W. A. 2008. Nanobubbles at the interface between water and a hydrophobic solid. *Langmuir*, 24, 4756–4764.

Zhao, H., Bhattacharjee, S., Chow, R., *et al.* 2008. Probing surface charge potentials of clay basal planes and edges by direct force measurements. *Langmuir*, 24 (22), 12899–12910.